

Kinetic Study of Liquid-Phase Glycerol Hydrodeoxygenation into 1,2-Propanediol over CuPd/TiO₂-Na

Alba N. Ardila A,* Erasmo Arriola-Villaseñor, Rolando Barrera-Zapata, José Hernández, and Gustavo A. Fuentes



Cite This: *ACS Omega* 2023, 8, 14907–14914



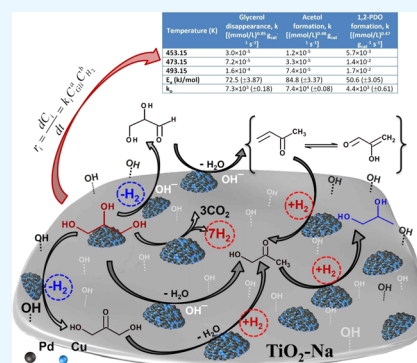
Read Online

ACCESS |

Metrics & More

Article Recommendations

ABSTRACT: Hydrodeoxygenation (HDO) kinetics of glycerol into 1,2-propanediol (1,2-PDO) in the liquid phase is studied on Cu-Pd/TiO₂ catalysts. At a stirring speed higher than 480 rpm and an average diameter of the catalyst particles smaller than 89.5 μm, no mass transfer resistance artifacts are observed. The increasing temperature and H₂ concentration promote the glycerol conversion and the selectivity to 1,2-PDO and disfavor the selectivity to acetol. Based on the experimental data, empirical kinetic pseudo-homogeneous expressions are proposed for glycerol disappearance, 1,2-PDO formation, and acetol formation in the catalytic system. Dependence of the disappearance rate of glycerol is closer to 1 with respect to glycerol and nonmeaningful with respect to H₂. The formation rate of 1,2-PDO is not highly dependent on the initial concentration of glycerol or H₂, and the formation rate of acetol is directly dependent on glycerol and inversely dependent on H₂, since it accelerates acetol conversion to 1,2-PDO. The activation energies for glycerol disappearance (77.8 kJ/mol), 1,2-PDO formation (51.2 kJ/mol), and acetol formation (84.6 kJ/mol) evidenced the selective formation of 1,2-PDO in this catalytic system.



INTRODUCTION

High amounts of glycerol are obtained as side products in the biodiesel production process. The relatively low price of glycerol affects the economic balance of the biodiesel production; however, it is possible to add value¹ by developing new glycerol-based catalytic processes, i.e., to produce industrially relevant chemicals such as 1,2-propanediol (1,2-PDO)^{2–4} used in many industries, including resins, pharmaceuticals, cosmetics, fragrances, and paints, among others. The annual production of 1,2-PDO is around 1 million tons only in the USA. The current industrial synthesis of 1,2-PDO involves hydrolysis of propylene oxide with water at temperatures between 125 and 200 °C and 2 MPa pressure.^{5,6} In the last few years, there have been many efforts aimed at the conversion of glycerol into 1,2-PDO by catalytic hydrodeoxygenation (HDO). In this way, Cu-based catalysts have been found to achieve high selectivity, but they are generally unstable.^{3,7–11} On the other side, catalysts with Pt-, Ru-, Au-, Ni-, or Rh-containing materials are also active catalysts for this process, but their selectivity toward 1,2-PDO is not good enough.^{10,12,13}

In the previous work, we report a catalyst, Cu-Pd/TiO₂ promoted by Na, for the valorization of glycerol using aqueous-phase HDO into 1,2-PDO.¹⁴ The catalysts proved to be highly active and overcome the typical drawbacks of Cu catalysts, i.e., the relatively low stability. We also demonstrated that the high selectivity to 1,2-PDO of the bimetallic catalysts synthesized is

due to the formation of CuPd alloy nanoparticles with sizes smaller than 6–7 nm with their surface enriched with Cu and basically made up of Cu⁰-Pd⁰ and Cu¹⁺-Pd⁰.¹⁵ However, according to our experimental observations and literature data, obtaining 1,2-PDO from glycerol is not an elementary reaction with 1,2-PDO as the only product formed in the reaction.^{9,14–20} Thus, depending on the reaction conditions, different intermediates and/or side products could affect the kinetics of the reaction and the selectivity to 1,2-PDO. Nevertheless, to use our catalyst in a specific industrial application for the production of 1,2-PDO from glycerol, it is necessary to understand the reaction mechanism and to know some kinetic models; moreover, to the best of our knowledge, these aspects have not been discussed in the previous studies.

Here, we report the influence of several reaction parameters for 1,2-PDO production from glycerol HDO on the aqueous phase over the Cu-Pd/TiO₂-Na catalyst. The parameters studied were temperature, H₂ concentration, and glycerol concentration. The effect of such parameters over reaction rates, glycerol conversion, 1,2-PDO selectivity, and hydrox-

Received: September 6, 2022

Accepted: January 25, 2023

Published: April 24, 2023



acetone (acetol) selectivity were analyzed. Acetol selectivity was included in the analysis because significant amounts of this substance are present in the reaction system as an apparent side product of the reaction; thus, such analysis could give insights into the mechanistic pathway of the 1,2-PDO formation from glycerol HDO in the aqueous phase over the Cu-Pd/TiO₂-Na catalyst. The aqueous-phase concentration of H₂ in the reaction system was determined by correlations with the literature-based data, while the equilibrium compositions for the glycerol + water mixtures were simulated in Aspen Plus. In addition, for accurate reaction rate measurements, the absence of internal mass transfer limitations was tested following the Weisz–Prater criterion.

EXPERIMENTAL SECTION

Catalyst Preparation. The Cu-Pd/TiO₂-Na catalyst (nominal atomic ratio Cu/Pd = 1.67) was prepared by sequential impregnation on TiO₂ (Degussa, P-25 powder). For this, 5%Na/TiO₂ was prepared by first treating TiO₂ with NaOH dissolved in methanol (5 mL of methanol/g of TiO₂). The loading of Pd and of Cu was set at 5 wt %. The details of the catalyst synthesis and activation procedure and the characterization results were published in the previous work.^{14,15}

Swelling Experiments. Swelling is a phenomenon commonly observed in different kinds of supported heterogeneous catalysts, especially when they are in contact with polar solvents.^{21,22} In liquid-phase kinetic studies, the relationship between swelling and the reaction mixture composition is important for adequate evaluation of diffusional mass transfer limitations, i.e., for determining the true radius of the catalyst particle in the Weisz–Prater criterion.²² The relationship between catalyst swelling and the reaction mixture composition was determined as follows: 0.1 g of the dry catalyst was placed in a glass cylinder (60 × 4.7 mm²), and after compacting by centrifugation, the solid height was measured (h_0); then, around 1.0 mL of the liquid mixture (Table 1) was

Table 1. Swelling of Cu-Pd/TiO₂-Na Catalysts

exp.	mass fraction (wt %)				%H
	water, W	glycerol, G	1,2-PDO, P	acetol, A	
1	0.974	0.206	0	0	6.3
2	0.715	0.084	0.077	0.124	0.8
3	0.772	0.046	0.158	0.024	6.3
4	0.483	0.138	0.198	0.181	13.5
5	0.711	0.020	0.180	0.089	14.3
6	0.583	0.317	0.100	0	19.3
7	0	1	0	0	36.1
8	0	0	1	0	18.0
9	0	0	0	1	23.0
10	1	0	0	0	12.2

added, and the final solid height (h_f) was measured after 13 days when no changes in the solid-phase height were observed. The percentage of swelling (%H) was estimated according to eq 1. Liquid mixtures were prepared including the main substances expected to be present in the reaction system: water, glycerol, 1,2-PDO, and acetol.

$$\%H = \frac{h_f}{h_0} \times 100\% \quad (1)$$

Catalyst Density. The density of the catalyst was determined by placing a known amount of the sample (0.2931 g) in a graduated cylinder containing 3 mL of water. Once the catalyst was fully swollen (around 13 days), the displaced volume of water was measured. This value was used as a rough estimate of the catalyst volume. Catalyst density was estimated as the ratio of the mass of the catalyst and the displaced volume.

Aqueous-Phase Concentration of H₂. For reaction rate estimation, it is necessary to determine the real H₂ concentration in the liquid phase. As far as we know, there are no available literature data related to H₂ solubility in water + glycerol liquid mixtures under reaction conditions of the present study. Thus, the H₂ concentration in the liquid phase was estimated as follows: using the Henry constant for H₂ in pure water at 25 °C (7.10×10^4 atm), the Henry constant for H₂ in pure water was estimated for different temperatures, i.e., 180, 200, and 220 °C, by means of the Van't Hoff equation (eq 2)

$$K_H(T) = K_H(T^\circ) \exp\left[-C\left(\frac{1}{T} - \frac{1}{T^\circ}\right)\right] \quad (2)$$

where T is the temperature (180, 200, and 220 °C), T° is the standard temperature (298.15 K), C is the constant for the gas in the solvent water (500 K), and $K_H(T^\circ)$ is the solubility constant for the gas in the solvent at the reference temperature (298.15 K).

In a similar way, the Henry constant for H₂ in pure glycerol at 25 °C (1.86×10^5 atm)^{21,23,24} was used for the estimation of the Henry constant of H₂ in pure glycerol at different temperatures. The Henry constant for binary mixtures was then calculated according to eq 3

$$\ln K_{H_2, \text{mix}} = X_1 \ln K_{H_2, \text{Glic}} + X_2 \ln K_{H_2, \text{Aqua}} - a_{1,2} X_1 X_2 \quad (3)$$

where $K_{H_2, \text{mix}}$ is the Henry constant for H₂ in the glycerol + water mixture; X_1 is the molar fraction for glycerol in the glycerol + water mixture; $K_{H_2, \text{Glic}}$ is the Henry constant for H₂ in pure glycerol at the desired temperature; X_2 is the molar fraction of water in the glycerol + water mixture; $K_{H_2, \text{Aqua}}$ is the Henry constant for H₂ in pure water at the desired temperature; and $a_{1,2}$ is the constant for solvent mixtures. $a_{1,2} = 0$ for ideal mixtures.

Simulated Equilibrium Compositions for the Glycerol + Water Mixtures. For the catalytic reactions (described in the next section), aqueous glycerol solutions are used in the reaction system and the H₂ pressure is 100 psi. The reaction temperature can reach 220 °C, with the autogenic pressure being up to 450 psi. Therefore, it is important to verify that the reaction is carried out in the liquid phase. In that sense, the equilibrium reaction mixture composition was estimated using Aspen Plus (V. 8.6) software. An equilibrium reactor (REquil) available in the built-in models of software was used. Algorithms associated with this reactor model are capable of predicting both chemical and phase equilibria.²³ Two inlet streams were simulated: one containing the aqueous mixture water + glycerol and the other one containing the H₂ input. As a basis for calculation, 10 mol/s for each stream was assumed. The system was simulated at 450 psi using NRTL as a thermodynamic model for LLE and SR equation of the state for VLE. Missing parameters were estimated by the UNIQUAC group contribution method.

Kinetic Experiments. Kinetic tests were carried out in a batch reactor (Parr Instruments); the total reactor volume was 320 mL. In a typical reaction, the reactor was loaded with 50 mL of a 20 wt % aqueous solution of glycerol and the catalyst (previously reduced) amount necessary. The catalysts were transferred from the reduction tube to the reactor, while trying to keep them in an inert atmosphere, but a brief exposure to air cannot be excluded. After the reactor was sealed, it was flushed with N₂ at 0.1 MPa for 5 min to remove air from the headspace. N₂ was subsequently flushed with H₂ at 0.1 MPa for 5 min. The reactor was then pressurized with H₂ (100 psi) and heated under moderate agitation (480 rpm) until the desired reaction temperature (220 °C). Once this temperature was reached, an initial liquid sample was drawn to mark the start of the reaction and the speed of agitation was increased. The reaction was allowed to proceed for 6 h, while the liquid phase was sampled each hour. The liquid reaction samples were analyzed by gas chromatography (Agilent 6850 GC equipped with a flame ionization detector (FID) and an HP-INNOWAX capillary column). The reaction products were also identified by GC-MS (Agilent 5975 GC-MS with a HP-PLOT Q column). Once the reactor was cooled to room temperature, the gas samples were collected from the headspace in gas-sampling bulbs and analyzed using two gas chromatographs equipped with thermal conductivity detectors (TCD): a Shimadzu GC-12A equipped with a Porapak Q packed column was used for detecting H₂ and an HP 5890 GC equipped with an HP-Plot Q capillary column was used for detecting light hydrocarbons, CO and CO₂. The kinetic data were obtained by the method of initial rates; the rate law and initial reaction rates were found using the differential method by fitting the experimental data of the reaction at conversion lower than 20%. Additionally, all the tests and reactions were performed in triplicate.

RESULTS AND DISCUSSION

Simulated Equilibrium Composition for the Reaction Mixture Water + Glycerol.

Table 2 shows the simulated

Table 2. Composition for the Reaction Mixtures Simulated in Aspen Plus

substance	molar fraction for the inlet streams		molar fraction for the outlet stream	
	liquid mixture	H ₂	vapor	liquid
water	0.95338	0	0.72321	0.94497
glycerol	0.04662	0	0.00033	0.05478
hydrogen	0	1	0.27646	0.00023

composition (molar fraction) expected for the reaction mixture under the reaction conditions. According to the simulation results, it can be observed that a higher amount of glycerol in the system is in the liquid phase, with the vapor-phase glycerol molar fraction being around 0.00033; thus, it can be expected that under the studied conditions, the reaction is carried out in the liquid phase.

Application of the Weisz–Prater Criterion. The Weisz–Prater criterion (eq 4) was used to verify the absence of intraparticle mass transfer limitations, where r_{obs} is the observed reaction rate of glycerol (mol/gcat·s), R is the “true radius” of the particle (cm), ρ_{part} is the particle density (g/cm³), De is the effective diffusivity of glycerol in the reaction

mixture (cm²/s), and C_i is the initial concentration of glycerol (mol/cm³).

$$\Phi = \frac{-r_{\text{obs}}R^2\rho_{\text{part}}}{De C_i} \quad (4)$$

The “true” particle radius (R) was determined from swelling experiments (Table 1). An empirical correlation between swelling (%H) and the mixture composition was obtained by multiple linear regression (eq 5). The correlation coefficient (0.87) is greater than that (0.46) reported elsewhere²⁴ in the study of esterification reactions over cation-exchange resins and closer to that reported elsewhere²² (0.92) in the study of epoxidation reactions over Amberlyst-based catalysts. Thus, R was calculated from eq 6, which is expected to give a good representation of the catalyst swelling phenomena. The R value obtained was 4.868×10^{-3} cm.

$$\%H = 4.32W + 35.31G + 18.08P + 22.07A \quad (5)$$

$$R = r_{\text{catalizador seco}} \left(1 + \frac{\%H}{100} \right) \quad (6)$$

Here, r is the radius of the dry catalyst (from Table 2).

The effective diffusion coefficient De (1.307×10^{-3} cm²/s) was determined by eq 7²²

$$De = D_{G-A} \frac{\varepsilon}{\tau} \quad (7)$$

where D_{G-A} is the diffusion coefficient for glycerol in water, estimated under the reaction conditions within software Aspen Plus, ε is the porosity (0.5688), estimated with eq 8 using a value of pore volume ($V_p = 0.45$ cm³/g) and a mass value ($m = 0.047$ g) from N₂ adsorption probes, and τ is the tortuosity factor (1.8352) estimated from eq 9. According to swelling probes, the average particle density ρ_{part} was estimated to be 2.931 g/cm³.

$$\varepsilon = \frac{m \times V_p}{m \times V_p + (m/\rho_{\text{part}})} \quad (8)$$

$$\tau = \frac{\varepsilon}{1 - \pi[(1 - \varepsilon)(3/4\pi)]^{2/3}} \quad (9)$$

Using an initial concentration of glycerol C_i of 2.22×10^{-3} mol/cm³, eq 4 returns a Weisz–Prater criterion of 1.3015×10^{-3} (0.69) for the catalyst of 89.5 μm average diameter (Fraction IV, Table 2). Thus, this particle size was used in further experiments for avoiding mass transfer limitations in the catalytic system. According to the criteria, if Φ (eq 4) is $\ll 1$, there are no diffusional artifacts on the reaction system. The value obtained was 4.034×10^{-4} .

Evaluation of Mass Transfer Resistances. The stirring speed was varied between 250 and 600 rpm (Figure 1) for determining external mass transfer resistances. Above 480 rpm, no effects on the initial reaction rate for glycerol HDO in the aqueous phase were observed. Thus, the stirring speed was set at 480 rpm for all further experiments to avoid external mass transfer resistances. The effect of internal diffusion on initial reaction rates was determined by measuring reaction rates for different average catalyst particle sizes (Table 2). It was observed that initial reaction rates did not vary with catalyst particle sizes for fraction III (average particle diameter, 115.0 μm) or fraction IV (average particle diameter, 8935 μm). The

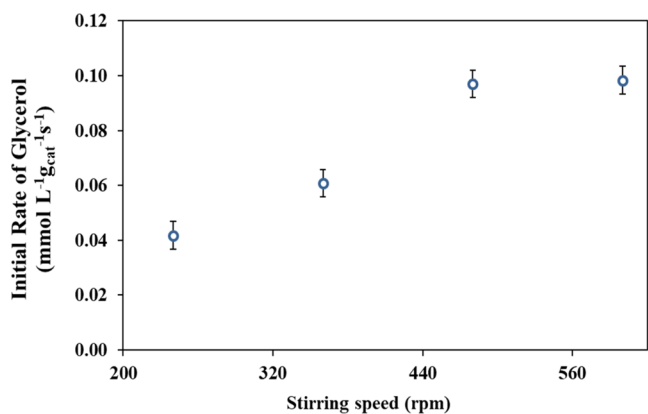


Figure 1. Effect of stirring speed on the initial reaction rate of glycerol HDO over Cu-Pd/TiO₂-Na catalysts. Aqueous glycerol 20 wt %; 50 mL; H₂ pressure: 100 psi; catalyst amount: 0.3 g; and temperature: 220 °C.

fraction used in further experiments was determined according to results observed for the Weisz–Prater criteria evaluation.

Effect of the Amount of the Catalyst on the Rate of the Initial Reaction of Glycerol. Figure 2 shows that there is

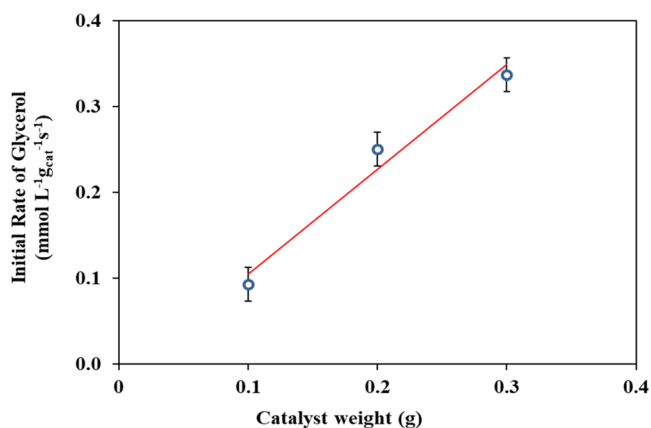


Figure 2. Effect of the catalyst loading on the initial rate of glycerol HDO. Aqueous glycerol 20 wt %; 50 mL; H₂ pressure: 100 psi; temperature: 220 °C; and stirring speed: 480 rpm.

a linear relationship between the amount of the catalyst and the initial rate of glycerol HDO in the range of mass of the catalyst studied. Similar results were obtained by Vasiliadou and Lemonidou;²⁵ they ensured that the variation of the catalyst weight between 0.05 and 0.35 g clearly shows a linear relation with the reaction rate, proving the absence of external mass transfer limitations (Table 3).

Effect of Reaction Temperature. The effect of temperature and concentration of the reaction mixture was investigated on the glycerol conversion and the product selectivity for glycerol HDO to 1–2 PDO in the aqueous phase. Figure 3 shows that both conversion of glycerol and 1,2-PDO selectivity are favored by increasing temperature, while selectivity to acetol and other products (including ethanol, methanol, *n*-propanol, acetaldehyde, propionaldehyde, acetone, ethylene glycol, acetic acid, and propionic acid, among others) tends to decrease with increasing temperature.

Effect of the Initial Concentration of H₂. H₂ concentration in the aqueous phase was estimated as described in the Experimental Section. Figure 4 shows that there is a

Table 3. Effect of Catalyst Particle Size on the Initial Reaction Rate of Glycerol HDO over Cu-Pd/TiO₂-Na Catalysts

fraction	particle size range (μm)	average diameter 2r dry catalyst (μm)	initial reaction rate ^a of glycerol HDO (mmol L ⁻¹ s ⁻¹ g _{cat} ⁻¹)
I	180–149	164.5	0.19
II	149–125	137.0	0.22
III	125–105	115.0	0.34
IV	105–74	89.5	0.34

^aAqueous glycerol 20 wt %; 50 mL; H₂ pressure: 100 psi; catalyst amount: 0.3 g; temperature: 220 °C; and stirring speed: 480 rpm.

linear correlation between the partial pressure of H₂ and H₂ concentration in the liquid phase. As observed in Figure 4, the correlation line does not cross the origin; thus, the partial pressure of H₂ required for getting an effective H₂ transference to the liquid phase should be at a lower limit (under 50 psi). Knowing if H₂ partial pressure or H₂ concentration in the liquid phase is the right choice is very necessary because we used the H₂ partial pressure in the rate expression and demonstrated that the dissolved amount of hydrogen is directly proportional to the partial pressure of hydrogen in the gas phase. Even more, considering the total amount of the substances in the reaction system, it can be observed that data for the simulated amount of H₂ in the liquid phase (see Table 2) are in good agreement with experimental data from Figure 4.

The effect of H₂ concentration on the reaction system was studied by varying the initial H₂ partial pressure between 50 and 200 psi; the other remaining reaction conditions were the same for all experiments. The resulting trends of glycerol conversion and product selectivity are like those observed with varying the reaction temperature, i.e., glycerol conversion increases, 1,2-PDO selectivity increases, and acetol selectivity decreases by increasing the initial concentration of H₂ (Figure 5). Similar results have been reported for different catalytic systems, which show that 1,2-PDO formation is favored at high H₂ pressures,^{26,27} while H₂ could act as an accelerator for acetol conversion to 1,2-PDO.^{19,28,29}

In the previous work,¹⁴ we report the conversion of glycerol in the absence of H₂ in the initial reaction mixture. The glycerol conversion under these conditions was ~39% and the major products identified in the liquid phase were acetol (69.4%) and 1,2-PDO (19.6%). In this set of experiments, it is possible to obtain these products due to the residual hydrogenation observed stemming from the H₂ generated through reforming; however, the conversion of acetol to 1,2-PDO was restricted by the limited availability of active hydrogen in the reaction medium; therefore, it was possible to determine the generation of reforming H₂ due to the presence of Pd in the catalyst, with which it was found that there is no limitation of H₂.

Effect of the Initial Concentration of Glycerol. The effect of the initial glycerol concentration was evaluated by varying the glycerol aqueous solution concentration between 20 and 40 wt %, with all remaining reaction conditions constant for all experiments. Results are shown in Figure 6. It can be seen that glycerol conversion diminishes with increasing initial concentration.

Vasiliadou et al.¹⁹ reported similar trends. However, they observed a decrease in the glycerol conversion by increasing its concentration from 80 to 100 wt %. Such behavior was

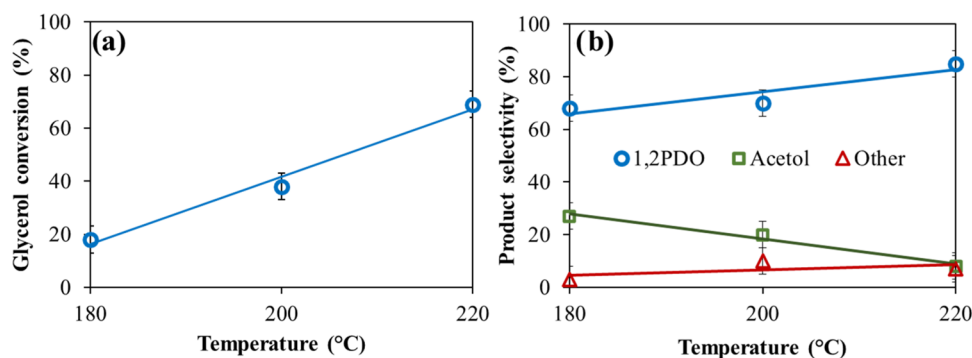


Figure 3. Glycerol HDO over Cu-Pd/TiO₂-Na catalysts at different temperatures. (a) Glycerol conversion; (b) product selectivity: ○ 1,2-PDO, □ acetol, and △ other. Reaction conditions: aqueous glycerol 20 wt %; 50 mL; H₂ pressure: 100 psi; catalyst amount: 0.3 g; average particle size diameter: 89.5 μm; temperature: 180–220 °C; stirring speed: 480 rpm; and reaction time 6 h. Other products include minor amounts of alcohols (ethanol, methanol (selectivity < 1%), and *n*-propanol) and traces of oxygenates such as acetaldehyde, propionaldehyde, acetone, ethylene glycol (selectivity < 2%), acetic acid, and propionic acid, which were identified by mass spectrometry.

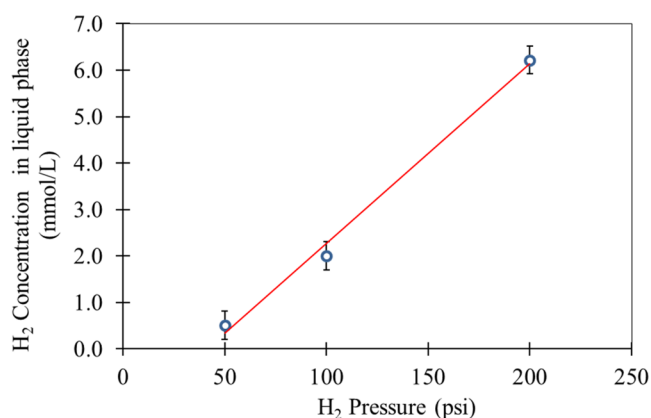


Figure 4. Correlation between partial pressure of H₂ and H₂ concentration in the liquid phase in aqueous glycerol solution (20 wt %) at 220 °C.

attributed to the increase in the mixture viscosity and to the increase in the molar ratio of glycerol/catalyst because there are a lower number of active sites available for the conversion of glycerol to 1,2-PDO. In the same way, Mane et al.⁷ observed an important reduction in glycerol conversion when its concentration was increased up to 60%wt. Notwithstanding, the authors did not observe important changes in product selectivity by increasing the glycerol concentration. In this study and according to Figure 6b, selectivity to 1,2-PDO

slightly decreases and selectivity to acetol increases by increasing the glycerol concentration in the reaction mixture.

Empirical Reaction Rates. According to our observations and based on the literature, glycerol HDO should include several simultaneous reactions; thus, the product profile will depend on the catalyst and reaction conditions. In general, two alternative pathways can facilitate glycerol HDO to 1,2-PDO in the aqueous phase over Cu catalysts: the glyceraldehyde route or the acetol one.^{3,5,6} When glycerol hydrogenolysis is carried out under basic conditions or in basic sites on the catalytic support, glycerol is dehydrogenated to glyceraldehyde, which is then dehydrated to 2-hydroxyacrolein on the basic sites and finally hydrogenated to 1,2-PDO on the metallic surface. In addition, glyceraldehyde can present a retroaldolization reaction and form glycolaldehyde and formaldehyde, which can be hydrogenated, producing ethylene glycol and methanol, respectively.^{30–38} Even more, direct breaking of the glycerol C–C bonds can lead to the formation of H₂, ethylene glycol, and methanol. Notwithstanding, the low selectivity observed for those products in our reaction system suggests that Cu-Pd/TiO₂-Na catalysts are not active for promoting C–C bond breaking; thus, no important additional formation of H₂ is expected through this pathway.¹⁴

According to the experimental observations of the present work, glycerol HDO to 1,2-PDO over Cu-Pd/TiO₂-Na catalysts in the liquid phase includes acetol as a main intermediate. In this pathway, acetol is formed by glycerol dehydration and then is hydrogenated, forming 1,2-PDO.³²

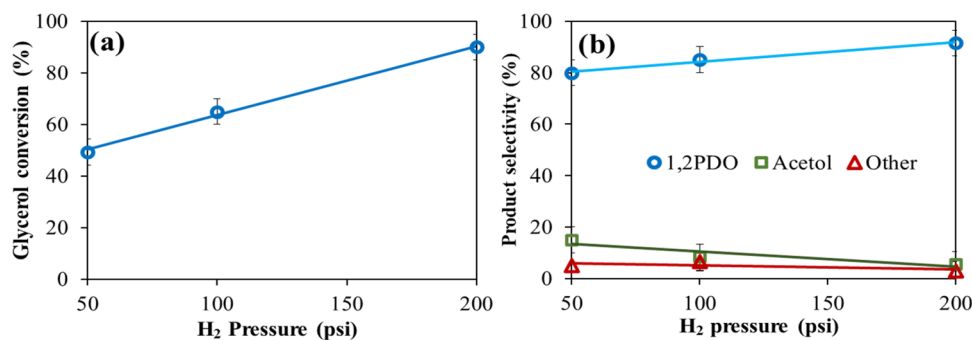


Figure 5. Glycerol HDO over Cu-Pd/TiO₂-Na catalysts at different H₂ pressures. (a) Glycerol conversion; (b) product selectivity: ○ 1,2-PDO, □ acetol, and △ other. Reaction conditions: aqueous glycerol 20 wt %; 50 mL; H₂ pressure: 50–200 psi; catalyst amount: 0.3 g; average particle size diameter: 89.5 μm; temperature: 220 °C; stirring speed: 480 rpm; and reaction time: 6 h.

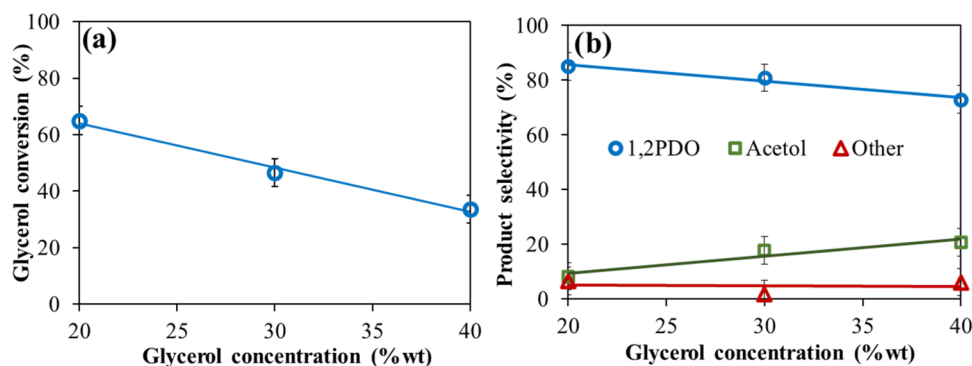


Figure 6. Glycerol HDO over Cu-Pd/TiO₂-Na catalysts at different H₂ pressures. (a) Glycerol conversion; (b) product selectivity: ○ 1,2-PDO, □ acetol, and △ other. Reaction conditions: aqueous glycerol (20, 30 or 40 wt %): 50 mL; H₂ pressure: 100 psi; catalyst amount: 0.3 g; average particle size diameter: 89.5 μm; temperature: 220 °C; stirring speed: 480 rpm; reaction time: 6 h.

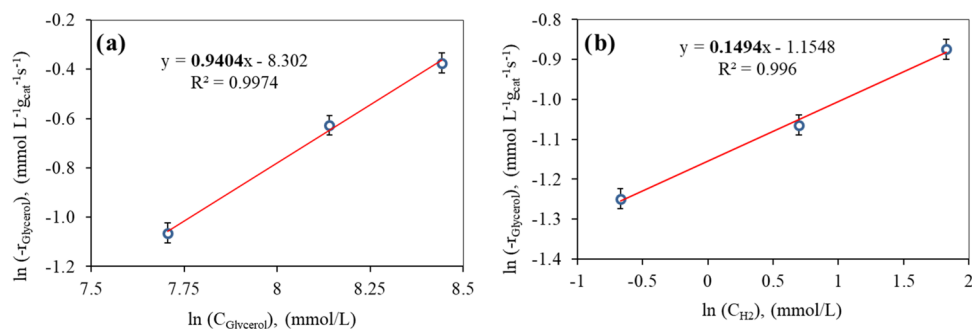


Figure 7. Apparent reaction order of glycerol disappearance with respect to glycerol (a) and with respect to H₂ (b).

Table 4. Kinetic Parameters for Glycerol, Acetol, and 1,2-PDO in the Glycerol HDO over Cu-Pd/TiO₂-Na Catalysts

temperature (K)	glycerol disappearance, k [(mmol/L) ^{0.85} g _{cat} ⁻¹ s ⁻¹]	acetol formation, k [(mmol/L) ^{0.48} g _{cat} ⁻¹ s ⁻¹]	1,2-PDO formation, k [(mmol/L) ^{0.47} g _{cat} ⁻¹ s ⁻¹]
453.15	3.0×10^{-5}	1.2×10^{-5}	5.7×10^{-3}
473.15	7.2×10^{-5}	3.3×10^{-5}	1.4×10^{-2}
493.15	1.6×10^{-4}	7.4×10^{-5}	1.7×10^{-2}
E_a (kJ/mol)	77.8 (±3.90)	84.6 (±3.40)	51.2 (±3.00)
k_0	8280 (±180)	20 650 (±800)	1510 (±610)

Because of the apparent complexity of the involved mechanistic pathway on the reaction system, a simple approximation to understand the kinetics is proposed: experimental data are adjusted to a power law model represented by eq 10, with i the representing glycerol, 1,2-PDO, or acetol and a and b being the apparent reaction order with respect to reactants, i.e., glycerol and hydrogen.

$$r_i = \frac{dC_i}{dt} = k_i C_{\text{Gly}}^a C_{\text{H}_2}^b \quad (10)$$

For the case of the glycerol disappearance rate, experimental data where glycerol concentration was varied and all remaining parameters were kept constant were used to determine the apparent reaction order with respect to glycerol (Figure 7a). In the same way, those experiments where H₂ concentration was varied and all remaining parameters were kept constant were used to determine the apparent reaction order with respect to H₂ (Figure 7b).

Figure 7a shows a linear correlation between the log value for the glycerol disappearance rate and its initial concentration. The apparent reaction order with respect to glycerol is 0.94. Other authors have reported values of 0.27, 0.5, and 0.72 for glycerol hydrogenolysis to 1,2-PDO using different catalytic

systems, Cu/SiO₂ or Ru/C catalysts, for example.^{28,39,40} The correlation in Figure 5b is also linear for the log value of glycerol disappearance rate and H₂ concentration. In this case, the apparent reaction order with respect to H₂ is 0.15; thus, the disappearance rate of glycerol has low dependence on the H₂ concentration. Vasiliadou and Lemonidou reported an apparent reaction order of 0.95 with respect to H₂ in the hydrogenolysis of glycerol to 1,2-PDO in the aqueous phase over the Cu/SiO₂ catalyst.²⁸

The reaction pseudo-constant k (eq 10) was estimated for different studied temperatures, and using the Arrhenius law, both the activation energy E_a and frequency factor k_0 were determined. The apparent activation energy estimated was 77.8 kJ/mol. Similar values have been reported for the glycerol hydrogenolysis to 1,2-PDO in the aqueous phase (65.5 and 77.1 kJ/mol) using Cu_{0.4}/Zn_{5.6-x}Mg_xAl₂O_{8.6} and Pd_xCu_{0.4}/Zn_{5.6-x}Mg_xAl₂O_{8.6-x} catalysts, respectively.^{32,41} Higher activation energies (96.8, 86.0, and 86.6 kJ/mol) have been reported for other catalytic systems.^{16,28,42,43} In the same fashion, kinetic power law expressions, activation energies, and frequency factors for the Arrhenius constant were calculated for the 1,2-PDO formation and for the acetol formation. Results are shown in Table 4.

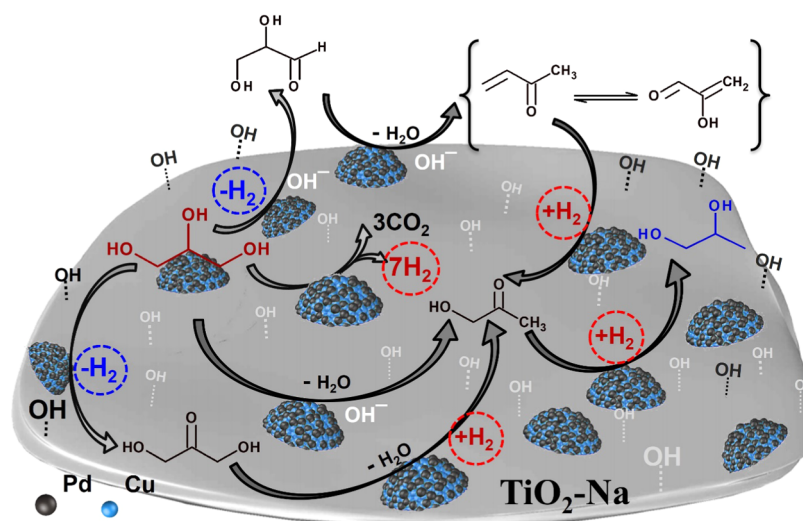


Figure 8. Reaction pathways for the formation of 1,2-PDO from glycerol by acetol routes under alkaline conditions.

Our results show that glycerol hydrodeoxygenation involves several consecutive and parallel reactions and the profile of products strongly depends on the catalyst, promoters, and reaction conditions used. In addition, our results reveal that the hydrogenolysis of glycerol to 1,2-PDO in the aqueous liquid phase can proceed mainly through the route with acetol as the main intermediate. Based on this, we propose three reaction routes that lead to the formation of acetol from glycerol (Figure 8). In the first route, the formation of acetol from the dehydration of glycerol can be considered. On the other hand, the formation of dehydrogenated intermediates such as glyceraldehyde or 1,3-di-hydroxyacetone rapidly from its dehydration and subsequent hydrogenation for the formation of acetol are other possible routes, where finally, the hydrogenation of acetol to 1,2-PDO would take place.

CONCLUSIONS

A Na-promoted bimetallic catalyst was developed for the aqueous-phase hydrodeoxygenation (HDO) of glycerol. The best results were obtained at 220 °C and 0.7 MPa H₂ with an initial turnover frequency (TOF based on Cu+Pd sites) of 0.14 s⁻¹ and a selectivity to 1,2-PDO of 85%. It was found that the increase in the concentration of H₂ in the liquid phase (in a range of 50–200 psi) positively affects the initial reaction speed of glycerol and 1,2-PDO formation, while decreasing the speed of acetol formation. On the other hand, the increase in reaction temperature (180–220 °C) positively affected the initial reaction speed of glycerol and the formation of both 1,2-PDO and acetol. In addition, the increase in the initial concentration of glycerol (20–40% by weight) resulted in a decrease in the glycerol conversion and the formation of 1,2-PDO slightly decreased and selectivity to acetol increased. Additionally, the experimental data were successfully adapted to a kinetic model of the simple power law applied to the global consumption of glycerol and to the global formation of acetol and 1,2-PDO.

AUTHOR INFORMATION

Corresponding Author

Alba N. Ardila A – Research Group in Environmental Catalysis and Renewable Energies, Facultad de Ciencias Básicas Sociales y Humanas, Politécnico Colombiano Jaime Isaza Cadavid

Isaza Cadavid, 050022 Medellín, Colombia; orcid.org/0000-0002-7675-0647; Email: anardila@elpoli.edu.co

Authors

Erasmio Arriola-Villaseñor – Research Group in Environmental Catalysis and Renewable Energies, Facultad de Ciencias Básicas Sociales y Humanas, Politécnico Colombiano Jaime Isaza Cadavid, 050022 Medellín, Colombia

Rolando Barrera-Zapata – CERES Research Group, Engineering Faculty, Chemical Engineering Department, Universidad de Antioquia, 050010 Medellín, Colombia; orcid.org/0000-0002-8718-9242

José Hernández – UPIIG, del Instituto Politécnico Nacional, 36275 Silao, Guanajuato, México

Gustavo A. Fuentes – Department of Process Engineering, Universidad A. Metropolitana-Iztapalapa, México DF 09310, Mexico; orcid.org/0000-0002-6010-6099

Complete contact information is available at:

<https://pubs.acs.org/10.1021/acsomega.2c05644>

Author Contributions

The article was written through contributions of all authors. All authors have given approval to the final version of the article.

Notes

The authors declare no competing financial interest.

ACKNOWLEDGMENTS

This research was made possible by the financial support of Universidad A. Metropolitana-Iztapalapa, México. A.N.A. acknowledges Politécnico Colombiano Jaime Isaza Cadavid.

ABBREVIATIONS

HDO, hydrodeoxygenation; 1,2-PDO, 1,2-propanediol; NRTL, nonrandom two liquids; UNIFAC, universal quasi-chemical

REFERENCES

(1) Pirzadi, Z.; Meshkani, F. From glycerol production to its value-added uses: A critical review. *Fuel* **2022**, 329, No. 125044.

- (2) Roy, D.; Subramaniam, B.; Chaudhari, R. V. Aqueous phase hydrogenolysis of glycerol to 1,2-propanediol without external hydrogen addition. *Catal. Today* **2010**, *156*, 31–37.
- (3) Yuan, Z.; Wang, J.; Wang, L.; et al. Biodiesel derived glycerol hydrogenolysis to 1,2-propanediol on Cu/MgO catalysts. *Bioresour. Technol.* **2010**, *101*, 7088–7092.
- (4) Md Rahim, S. A. N.; Lee, C. S.; Abnisa, F.; et al. Activated carbon-based electrodes for two-steps catalytic/ electrocatalytic reduction of glycerol in Amberlyst-15 mediator. *Chemosphere* **2022**, *295*, 133949.
- (5) Balaraju, M.; Jagadeeswaraiiah, K.; Prasad, P. S. S.; Lingaiah, N. Catalytic hydrogenolysis of biodiesel derived glycerol to 1,2-propanediol over Cu–MgO catalysts. *Catal. Sci. Technol.* **2012**, *2*, 1967–1976.
- (6) Meher, L. C.; Gopinath, R.; Naik, S. N.; Dalai, A. K. Catalytic hydrogenolysis of glycerol to propylene glycol over mixed oxides derived from a hydrotalcite-type precursor. *Ind. Eng. Chem. Res.* **2009**, *48*, 1840–1846.
- (7) Mane, R. B.; Hengne, A. M.; Ghalwadkar, A. A.; et al. Cu:Al nano catalyst for selective hydrogenolysis of glycerol to 1,2-propanediol. *Catal. Letters* **2010**, *135*, 141–147.
- (8) Yuan, Z.; Wu, P.; Gao, J.; et al. Pt/solid-base: A predominant catalyst for glycerol hydrogenolysis in a base-free aqueous solution. *Catal. Lett.* **2009**, *130*, 261–265.
- (9) Gabrysch, T.; Muhler, M.; Peng, B. The kinetics of glycerol hydrodeoxygenation to 1,2-propanediol over Cu/ZrO₂ in the aqueous phase. *Appl. Catal., A* **2019**, *576*, 47–53.
- (10) Miao, G.; Shi, L.; Zhou, Z.; et al. Catalyst design for selective hydrodeoxygenation of glycerol to 1,3-propanediol. *ACS Catal.* **2020**, *10*, 15217–15226.
- (11) Lin, Z.; Ammal, S. C.; Denny, S. R.; et al. Unraveling Unique Surface Chemistry of Transition Metal Nitrides in Controlling Selective C–O Bond Scission Pathways of Glycerol. *JACS Au* **2022**, *2*, 367–379.
- (12) Amada, Y.; Shinmi, Y.; Koso, S.; et al. Reaction mechanism of the glycerol hydrogenolysis to 1,3-propanediol over Ir-ReOx/SiO₂ catalyst. *Appl. Catal., A* **2011**, *105*, 117–127.
- (13) Greish, A. A.; Finashina, E. D.; Tkachenko, O. P.; et al. Hydrodeoxygenation of glycerol into propanols over a Ni/WO₃–TiO₂ catalyst. *Mendeleev Commun.* **2020**, *30*, 119–120.
- (14) Ardila, A. N.; Sánchez-Castillo, M. A.; Zepeda, T. A.; Villa, A. L.; Fuentes, G. A. Glycerol hydrodeoxygenation to 1,2-propanediol catalyzed by CuPd/TiO₂-Na. *Appl. Catal., A* **2017**, *219*, 658–671.
- (15) Ardila, A. N.; Arriola-Villaseñor, E.; Fuentes, G. A. Nature and Distribution of Cu and Pd Species in CuPd/TiO₂-Na Bimetallic Catalysts for Glycerol Hydrodeoxygenation. *ACS Omega* **2020**, *5*, 19497–19505.
- (16) Xi, Y.; Holladay, J. E.; Frye, J. G.; et al. A kinetic and mass transfer model for glycerol hydrogenolysis in a trickle-bed reactor. *Org. Process Res. Dev.* **2010**, *14*, 1304–1312.
- (17) Torres, A.; Roy, D.; Subramaniam, B.; Chaudhari, R. V. Kinetic modeling of aqueous-phase glycerol hydrogenolysis in a batch slurry reactor. *Ind. Eng. Chem. Res.* **2010**, *49*, 10826–10835.
- (18) Yfanti, V. L.; Lemonidou, A. A. Mechanistic study of liquid phase glycerol hydrodeoxygenation with in-situ generated hydrogen. *J. Catal.* **2018**, *368*, 98–111.
- (19) Vasiliadou, E. S.; Lemonidou, A. A. Kinetic study of liquid-phase glycerol hydrogenolysis over Cu/SiO₂ catalyst. *Chem. Eng. J.* **2013**, *231*, 103–112.
- (20) Bouriakova, A.; Mendes, P. S. F.; Katryniok, B.; De Clercq, J.; Thybaut, J. W. Co-metal induced stabilization of alumina-supported copper: impact on the hydrogenolysis of glycerol to 1,2-propanediol. *Catal. Commun.* **2020**, *146*, 106134.
- (21) Barrera Zapata, R.; Villa, A. L.; Montes De Correa, C. Limonene epoxidation: Diffusion and reaction over PW-Amberlite in a triphasic system. *Ind. Eng. Chem. Res.* **2006**, *45*, 4589–4596.
- (22) Pääkkönen, P. K.; Krause, A. O. I. Diffusion and chemical reaction in isoamylene etherification within a cation-exchange resin. *Appl. Catal., A* **2003**, *245*, 289–301.
- (23) Jungermann, E.; Norman, S. *Glycerine: A Key Cosmetic Ingredient*; Routledge, 1991.
- (24) Segur, J. Physical properties of glycerol and its solutions. *Glycerol* **1953**, *2*, 347–348.
- (25) Vasiliadou, E. S.; Lemonidou, A. A. Kinetic study of liquid-phase glycerol hydrogenolysis over Cu/SiO₂ catalyst. *Chem. Eng. J.* **2013**, *231*, 103–112.
- (26) Plus, A. *Aspen Plus 7.10. Methods*.
- (27) Huang, L.; Zhu, Y.; Zheng, H.; Ding, G.; Li, Y. Direct conversion of glycerol into 1,3-propanediol over Cu-H₄SiW₁₂O₄₀/SiO₂ in vapor phase. *Catal. Lett.* **2009**, *131*, 312–320.
- (28) Huang, L.; Zhu, Y.; Zheng, H.; Li, Y. W.; Zeng, Z. Y. Continuous production of 1,2-propanediol by the selective hydrogenolysis of solvent-free glycerol under mild conditions. *J. Chem. Technol. Biotechnol.* **2008**, *83*, 1670–1675.
- (29) Reynoso, A. J.; Iriarte-Velasco, U.; Gutiérrez-Ortiz, M. A.; Ayastuy, J. L. Ce-doped cobalt aluminate catalysts for the glycerol hydrodeoxygenation (HDO) with in-situ produced hydrogen. *J. Environ. Chem. Eng.* **2022**, *10*, 107612.
- (30) Sharma, R. V.; Kumar, P.; Dalai, A. K. Selective hydrogenolysis of glycerol to propylene glycol by using Cu:Zn:Cr:Zr mixed metal oxides catalyst. *Appl. Catal., A* **2014**, *477*, 147–156.
- (31) Dasari, M. A.; Kiatsimkul, P. P.; Sutterlin, W. R.; Suppes, G. J. Low-pressure hydrogenolysis of glycerol to propylene glycol. *Appl. Catal., A* **2005**, *281*, 225–231.
- (32) Jin, X.; Dang, L.; Lohrman, J.; et al. Lattice-matched bimetallic CuPd-graphene nanocatalysts for facile conversion of biomass-derived polyols to chemicals. *ACS Nano* **2013**, *7*, 1309–1316.
- (33) Xia, S.; Yuan, Z.; Wang, L.; Chen, P.; Hou, Z. Hydrogenolysis of glycerol on bimetallic Pd-Cu/solid-base catalysts prepared via layered double hydroxides precursors. *Appl. Catal., A* **2011**, *403*, 173–182.
- (34) Huang, Z.; Cui, F.; Kang, H.; Chen, J.; Xia, C. Characterization and catalytic properties of the CuO/SiO₂ catalysts prepared by precipitation-gel method in the hydrogenolysis of glycerol to 1,2-propanediol: Effect of residual sodium. *Appl. Catal., A* **2009**, *366*, 288–298.
- (35) Wu, Z.; Mao, Y.; Song, M.; Yin, X.; Zhang, M. Cu/boehmite: A highly active catalyst for hydrogenolysis of glycerol to 1,2-propanediol. *Catal. Commun.* **2013**, *32*, 52–57.
- (36) Wang, Y.; Qu, J.; Liu, H. Effect of liquid property on adsorption and catalytic reduction of nitrate over hydrotalcite-supported Pd-Cu catalyst. *J. Mol. Catal. A Chem.* **2007**, *272*, 31–37.
- (37) Pompeo, F.; Santori, G. F.; Nichio, N. N. Hydrogen production by glycerol steam reforming with Pt/SiO₂ and Ni/SiO₂ catalysts. *Catal. Today* **2011**, *172*, 183–188.
- (38) Peng, B.; Zhao, C.; Mejia-Centeno, I.; et al. Comparison of kinetics and reaction pathways for hydrodeoxygenation of C 3 alcohols on Pt/Al₂O₃. *Catal. Today* **2012**, *183*, 3–9.
- (39) Wawrzetz, A.; Peng, B.; Hrabar, A.; et al. Towards understanding the bifunctional hydrodeoxygenation and aqueous phase reforming of glycerol. *J. Catal.* **2010**, *269*, 411–420.
- (40) Lahr, D. G.; Shanks, B. H. Effect of sulfur and temperature on ruthenium-catalyzed glycerol hydrogenolysis to glycols. *J. Catal.* **2005**, *232*, 386–394.
- (41) Lahr, D. G.; Shanks, B. H. Kinetic analysis of the hydrogenolysis of lower polyhydric alcohols: glycerol to glycols. *Ind. Eng. Chem. Res.* **2003**, *42*, 5467–5472.
- (42) Xia, S.; Nie, R.; Lu, X.; et al. Hydrogenolysis of glycerol over Cu₂O/Zn₅6-xMgxAl₂O_{8.6} catalysts: The role of basicity and hydrogen spillover. *J. Catal.* **2012**, *296*, 1–11.
- (43) Zhou, Z.; Li, X.; ZENG, T.; et al. Kinetics of hydrogenolysis of glycerol to propylene glycol over Cu-ZnO-Al₂O₃ catalysts. *Chinese J. Chem. Eng.* **2010**, *18*, 384–390.